

Amorphous Si/SiO₂ distributed Bragg reflectors with transfer printed single-crystalline Si nanomembranes

Minkyu Cho, Jung-Hun Seo, Deyin Zhao, Jaeseong Lee, Kanglin Xiong, Xin Yin, Yonghao Liu, Shih-Chia Liu, Munho Kim, Tong J. Kim, Xudong Wang, Weidong Zhou, and Zhenqiang Ma

Citation: *Journal of Vacuum Science & Technology B* **34**, 040601 (2016); doi: 10.1116/1.4945998

View online: <http://dx.doi.org/10.1116/1.4945998>

View Table of Contents: <http://scitation.aip.org/content/avs/journal/jvstb/34/4?ver=pdfcov>

Published by the AVS: Science & Technology of Materials, Interfaces, and Processing

Articles you may be interested in

[Ultra-thin distributed Bragg reflectors via stacked single-crystal silicon nanomembranes](#)

Appl. Phys. Lett. **106**, 181107 (2015); 10.1063/1.4921055

[SiO₂/TiO₂ distributed Bragg reflector near 1.5 \$\mu\$ m fabricated by e-beam evaporation](#)

J. Vac. Sci. Technol. A **31**, 061514 (2013); 10.1116/1.4823705

[Single-crystal silicon/silicon dioxide multilayer heterostructures based on nanomembrane transfer](#)

Appl. Phys. Lett. **90**, 183107 (2007); 10.1063/1.2734367

[High-reflectance III-nitride distributed Bragg reflectors grown on Si substrates](#)

Appl. Phys. Lett. **87**, 241103 (2005); 10.1063/1.2140874

[Si wafer bonded of a - Si/a - Si N x distributed Bragg reflectors for 1.55 - \$\mu\$ m -wavelength vertical cavity surface emitting lasers](#)

J. Appl. Phys. **98**, 043107 (2005); 10.1063/1.2009075



SHIMADZU
Excellence in Science

Powerful, Multi-functional UV-Vis-NIR and FTIR Spectrophotometers

Providing the utmost in sensitivity, accuracy and resolution for a wide array of applications in materials characterization and nanotechnology research

- Photovoltaics
- Polymers
- Thin films
- Paints/inks
- Ceramics
- FPDs
- Coatings
- Semiconductors

[Click here to learn more](#)



LETTERS

Amorphous Si/SiO₂ distributed Bragg reflectors with transfer printed single-crystalline Si nanomembranes

Minkyu Cho^{a)} and Jung-Hun Seo

Department of Electrical and Computer Engineering, University of Wisconsin-Madison, Madison, Wisconsin 53706

Deyin Zhao

Department of Electrical Engineering, University of Texas at Arlington, Texas 76019

Jaeseong Lee and Kanglin Xiong

Department of Electrical and Computer Engineering, University of Wisconsin-Madison, Madison, Wisconsin 53706

Xin Yin

Department of Material Science and Engineering, University of Wisconsin-Madison, Madison, Wisconsin 53706

Yonghao Liu and Shih-Chia Liu

Department of Electrical Engineering, University of Texas at Arlington, Texas 76019

Munho Kim and Tong J. Kim

Department of Electrical and Computer Engineering, University of Wisconsin-Madison, Madison, Wisconsin 53706

Xudong Wang

Department of Material Science and Engineering, University of Wisconsin-Madison, Madison, Wisconsin 53706

Weidong Zhou^{b)}

Department of Electrical Engineering, University of Texas at Arlington, Texas 76019

Zhenqiang Ma^{b)}

Department of Electrical and Computer Engineering, University of Wisconsin-Madison, Madison, Wisconsin 53706

(Received 3 February 2016; accepted 30 March 2016; published 12 April 2016)

A distributed Bragg reflector (DBR) consisting of a single-crystal Si nanomembrane (NM) layer formed by the transfer printing technique on top of an evaporated amorphous Si (a-Si)/SiO₂ DBR structure was demonstrated. The reflectivity of different DBR structures/pairs is measured and verified it by the simulation. An improved surface roughness of the top layer by employing a Si NM suggests that the smoother single crystalline surface not only minimizes light scattering loss but also can be an epitaxial template layer for subsequent Si growth without contributing any strain. The results indicate a simple pathway toward achieving high performance Si/SiO₂ DBRs employing Si NM as a top layer. This method could also lead to the fabrication of large-area, high performance NM based DBRs at low cost with high throughput. © 2016 American Vacuum Society. [<http://dx.doi.org/10.1116/1.4945998>]

I. INTRODUCTION

Distributed Bragg reflector (DBR) is one of the most important photonic components that are used in a wide range of applications such as vertical cavity surface emitting lasers,^{1–5} resonant cavity light-emitting diodes and photodetectors,^{6–9} solar cells, etc.^{10,11} Si and SiO₂ are attractive

material choices for DBR in infrared optoelectronics due to the high index contrast¹⁰ and the capability of monolithic integration with Si CMOS chips for silicon photonics. Typically, Si/SiO₂ DBR was fabricated either by chemical vapor deposition, pulse laser deposition,¹² or atomic layer deposition.¹³ However, these deposition methods can only provide either amorphous or polycrystalline layers, and limit the performance improvement due to light scattering at interfaces or grain boundaries. On the other hand, single-crystalline Si offers well-ordered and smooth film quality that minimizes light scattering, and thus is one of the ideal DBR materials for near-infrared applications. However, it is

^{a)}Present address: Department of Mechanical Engineering, Korea Advanced Institute of Science and Technology (KAIST), 291 Daehak-ro, Yuseong-gu, Daejeon 305-701, South Korea.

^{b)}Authors to whom correspondence should be addressed; electronic addresses: wzhou@uta.edu and mazq@engr.wisc.edu

technically difficult to realize the single crystalline Si based Si/SiO₂ DBR due to the physical limitations in single crystal growth. Such a single crystalline Si/SiO₂ DBR was only possible by a series of ion implantations, wafer bonding, or back side wrapping processes. However, the performance was limited due to the limited interface qualities in these non-crystalline Si based DBRs. Recently, based on the nanomembrane (NM) transfer printing method, single-crystal Si NM/SiO₂ DBRs have been demonstrated with the improved interface quality and promising performance.^{14,15} This method requires several times of NM stacking and Si thermal oxidation, which implies high processing cost. A simplified method of forming high performance Si/SiO₂ DBR is thus desired.

In this work, we report a hybrid DBR structure, where the multilayer deposited amorphous Si (a-Si)/SiO₂ DBR was completed for the majority of the layers, followed by only one layer of transfer printed single crystalline Si NM. For most DBR applications, because the few layers next to the optical cavity are most critical as the field concentration is higher in these layers, replacing one or top few layers of DBR structure with low loss, high quality single crystalline layer will result in improved optical properties. Si NM is expected to significantly reduce the overall scattering and absorption losses associated with the complete DBR structures. Here, we demonstrate a-Si/SiO₂ DBR with the top Si NM (namely, the DBR consists of 3.5 pairs of a-Si/SiO₂ and one Si NM layer transferred on top of it) via the transfer printing method. The measured reflectivity is higher than 98%. To verify the improvement in reflectivity in DBR by employing a single crystalline Si NM layer, four different samples prepared with and without top crystalline Si NM were fabricated and characterized. Surface roughness, crystal quality, and the strain in the transferred single-crystal Si NM layer were analyzed by an atomic force microscopy (AFM), an x-ray diffraction (XRD), and a Raman spectroscopy, respectively, to correlate the reflectivity with the surface condition of the last layer and its viability as an epitaxial growth template and high quality photonic layer.

II. EXPERIMENT

The fabrication process began with deposition of electron beam evaporated of SiO₂ layer on a (100) Si substrate followed by the deposition of a-Si layer by the same method. These deposition steps were repeated until the desired number of pairs of the a-Si/SiO₂ structure was obtained, as shown in Figs. 1(d) and 1(e). The thickness of each layer a-Si/SiO₂ in the 3.5-pairs DBR was 270/105 nm, respectively. Silicon-on-insulator (SOI) wafer with a 340 nm thick top Si layer and a 2000 nm thick buried oxide layer was prepared and thermally oxidized to reduce the thickness of the top Si layer down to 105 nm, followed by the removal of the top oxide layer by concentrated hydrofluoric acid (HF, 49%). The SOI wafer was patterned with a standard photolithography method and etched by a reactive ion etcher to define square shaped Si NMs [Fig. 1(a)]. After patterning the Si NM, the sample was immersed in HF solution to release

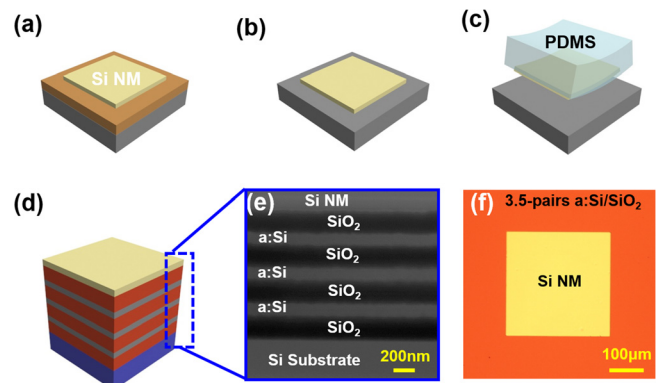


Fig. 1. (Color online) Illustrations of the fabrication process for a DBR with four-pairs deposited a-Si/SiO₂ layers and one top single-crystal Si NM layer printed on the deposited a-Si/SiO₂ pairs. (a) Patterning of Si NM on SOI. (b) Si NM release after the removal of buried oxide layer. (c) Si NM attached to PDMS stamp. (d) Transferred Si NM on top of the 3.5 pairs of deposited a-Si/SiO₂ layers. (e) An SEM cross-sectional image. (f) An optical microscope image of the finished DBR.

Si NMs from the SOI substrate [Fig. 1(b)]. The released single crystal Si NM was picked up by the polydimethylsiloxane (PDMS) stamp and transferred onto the 3.5-pairs a-Si/SiO₂ structures, as shown in Fig. 1(c). More detail fabrication process descriptions for NM releasing/transferring can be found elsewhere.^{16,17} After finishing the transfer, the DBR was annealed at 250 °C for 5 min in a rapid thermal annealing system to enhance bonding at the transferred interface. The completed DBR with a top single crystal Si NM layer is shown in Fig. 1(d). Figures 1(e) and 1(f) show a cross sectional scanning electron microscope (SEM) image and an optical of the finished 300 × 300 μm² DBR. It is noted that the cross sectional SEM image shown in Fig. 1(e) clearly shows the smoothness of the transferred Si NM layer.

III. RESULTS AND DISCUSSION

In order to investigate the optical properties with and without the transferred top Si NM layer, four test structures were prepared: (1) four-pairs a-Si/SiO₂ DBR, (2) Si NM-terminated four-pairs a-Si/SiO₂ DBR, (3) five-pairs a-Si/SiO₂ DBR, and (4) Si NM-terminated five-pairs a-Si/SiO₂. Prior to the optical characterizations, the surface roughness after each deposition/transfer was characterized using an AFM. The surface roughness after the 3.5-pairs a-Si and SiO₂ deposition were 3.67–4.26 nm, respectively, as shown in Fig. 2(a). Such values are nearly ten times larger than the values obtained from the typical polished Si wafer. The same surface characterization was carried out after transferring Si NM on top of the 3.5-pairs a-Si/SiO₂ structure. It is found that the top surface roughness was 0.265 nm after the Si NM transfer, which is similar to the roughness of polished Si wafer. This suggests that the realization of the higher reflection compact DBRs by incorporating Si NM can be globally applied to realize thinner DBRs by using less pairs, although the number of pairs in DBRs requires more evaporated layers in the conventional method. Raman spectroscopy studies were employed to investigate the strain on the Si NM layer after the transfer printing and thermal annealing

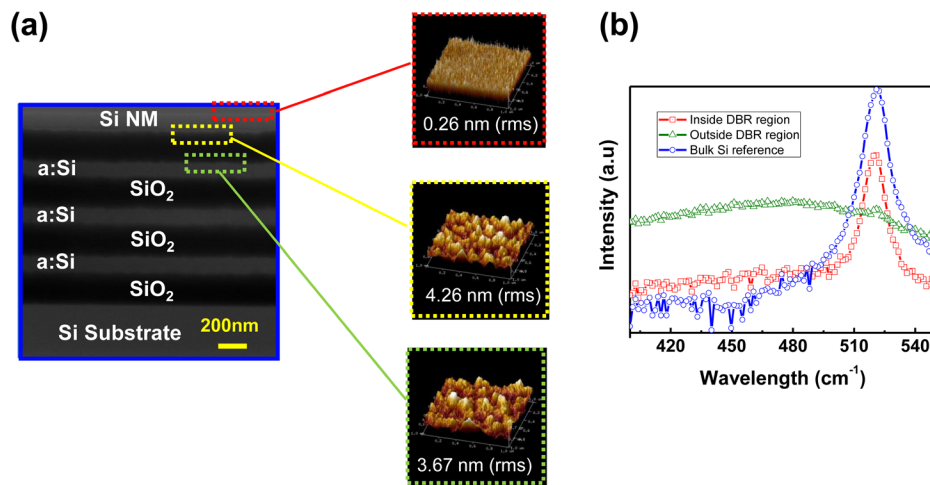


FIG. 2. (Color online) (a) AFM results indicating surface roughness at different process steps: surface profile (bottom) after third a-Si deposition, (center) after SiO₂ deposition, and (top) after Si NM transfer. (b) Raman spectra taken from (red square) the transferred Si NM region on DBR, (blue circle) Si bulk substrate, and (green triangle) outside of Si NM region on DBR.

processes on the Si NM-terminated DBR sample. Raman spectra were taken using a Horiba LabRAM ARAMIS Raman confocal microscope with an 18.5 mW blue laser (438 nm), using its low penetration depth to eliminate the effect by a phonon vibration from the Si substrate.

As shown in Fig. 2(b), the Si peak from the Si NM is located at 520 cm⁻¹, which corresponds to the Raman characteristic peak of bulk Si. This implies that no noticeable strain was created during the transfer process or on the Si NM layer and suggests that the top Si NM layer can be an epitaxial template layer for other Si epitaxial growth without producing any strain.¹⁸ The improved surface roughness was confirmed by the AFM images. To verify the optical performance of various multilayered DBR structures with and without top Si NM layer, reflectivity of each structure was measured, as shown in Fig. 3. The maximum reflectivities of

94.3%, 98%, 97.2%, and 98.5% were measured from four-pairs a-Si/SiO₂ DBR, Si NM-terminated four-pairs a-Si/SiO₂ DBR, five-pairs a-Si/SiO₂ DBR, and Si NM-terminated five-pairs a-Si/SiO₂ DBR, respectively. Interestingly, a much wider bandwidth (nearly 100–200 nm wider) was observed from the DBR with the top Si NM layer, which is attributed to the stronger field concentrated at the top Si NM layer than the a-Si layer. A reflectivity simulation with MIT electromagnetic equation propagation using a finite-difference time domain was performed to further verify the measured reflectivity.¹⁹ The measured material parameters of a-Si ($n = 2.3$) and single crystal Si ($n = 3.5$) and surface roughness values were incorporated in the simulations and the simulated results agree well with the measured results. While further optimization to improve the reflectivity is possible, it should be noted that the main purpose of the measurement is to verify the transferred/deposited multilayer structures as a result of optical interferences in the structures.

The crystal quality of transferred Si NM was characterized by XRD. Si NM transferred onto a glass substrate was prepared to minimize the background noise. Figure 4(a) shows an omega/2theta scan to measure the thickness, and a layer thickness of 110 nm was extracted from the thickness fringe spacing. Full width at half maximum (FWHM) was measured from a rocking curve scan, as shown in Fig. 4(b),

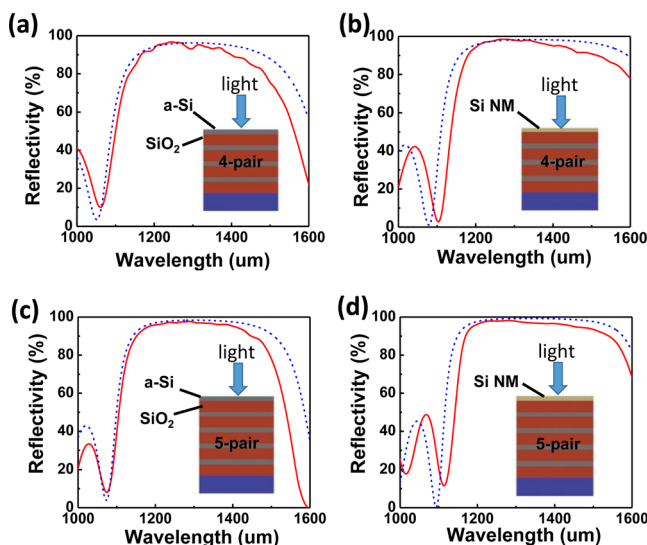


FIG. 3. (Color online) Measured (red solid line) and simulated (blue dash) reflection spectra of (a) four-pairs a-Si/SiO₂ DBR, (b) Si NM-terminated four-pairs a-Si/SiO₂ DBR, (c) five-pairs a-Si/SiO₂ DBR, and (d) Si NM-terminated five-pairs a-Si/SiO₂ DBR.

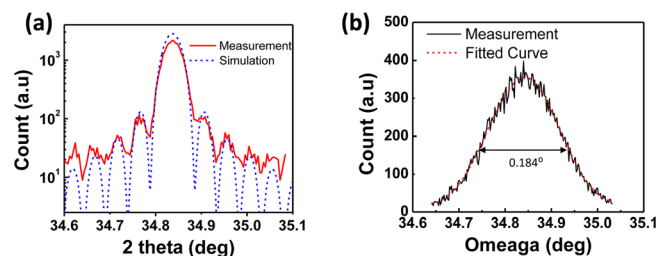


FIG. 4. (Color online) (a) Results of XRD omega/2theta scan for the transferred Si NM on a quartz substrate (red solid line). The calculation indicates 110 nm thickness for the Si NM (blue dash). (b) Omega scan of transferred Si NM. FWHM is 0.184°.

to demonstrate a high quality single-crystal Si layer. A FWHM value of 0.184° confirmed that the crystallinity of Si NM layer remained unchanged after the transfer-printing and following thermal annealing processes.

IV. CONCLUSION

In summary, a DBR consisting of only one layer of single-crystal Si NM that is transfer printed on top of an evaporated amorphous Si (a-Si)/SiO₂ DBR structure was demonstrated. A high reflectivity of 98.5% and bandwidth of 400 nm (>90%) at the near infrared (~1.3 μm) region were achieved from the five-pairs Si NM-terminated a-Si/SiO₂ DBR, which is due to the low absorption and smooth surface of single-crystal Si NM layer. An improved surface roughness of the top layer by employment of Si NM suggests that the smoother single crystalline surface not only reduces light scattering and loss but can also be an epitaxial template layer for other Si growth without production of strain. The fabrication approach is expected to reduce the process complexity and thus cost of Si/SiO₂-based DBRs.

ACKNOWLEDGMENTS

The work was supported by AFOSR under a PECASE Grant No. FA9550-09-1-0482. The program manager is Gernot Pomrenke.

- ¹F. Koyama, *J. Lightwave Technol.* **24**, 4502 (2006).
- ²J. Boucart *et al.*, *IEEE Photonics Technol. Lett.* **11**, 629 (1999).
- ³A. Ramakrishnan, G. Steinle, D. Supper, C. Degen, and G. Ebbinghaus, *Electron. Lett.* **38**, 322 (2002).
- ⁴G. Steinle, H. Riechert, and A. Y. Egorov, *Electron. Lett.* **37**, 93 (2001).
- ⁵W. Yuen *et al.*, *Electron. Lett.* **36**, 1121 (2000).
- ⁶O. I. Dosunmu, D. D. Cannon, M. K. Emsley, L. C. Kimerling, and M. S. Unlu, *IEEE Photonics Technol. Lett.* **17**, 175 (2005).
- ⁷M. K. Emsley, O. Dosunmu, and M. S. Unlu, *IEEE Photonics Technol. Lett.* **14**, 519 (2002).
- ⁸S. Collin, F. Pardo, and J.-L. Pelouard, *Appl. Phys. Lett.* **83**, 1521 (2003).
- ⁹E. F. Schubert, Y. H. Wang, A. Y. Cho, L. W. Tu, and G. J. Zydzik, *Appl. Phys. Lett.* **60**, 921 (1992).
- ¹⁰L. Zeng, Y. Yi, C. Hong, J. Liu, N. Feng, X. Duan, L. C. Kimerling, and B. A. Alamariu, *Appl. Phys. Lett.* **89**, 111111 (2006).
- ¹¹P. A. Snow, E. K. Squire, P. S. J. Russell, and L. T. Canham, *J. Appl. Phys.* **86**, 1781 (1999).
- ¹²J. Sellmann, C. Sturm, R. Schmidt-Grund, C. Czekalla, J. Lenzner, H. Hochmuth, B. Rheinländer, M. Lorenz, and M. Grundmann, *Phys. Status Solidi C* **5**, 1240 (2008).
- ¹³C. Hongjun, G. Hao, Z. Peiyuan, Z. Xiong, L. Honggang, W. Shengkai, and C. Yiping, *Appl. Phys. Express* **6**, 022101 (2013).
- ¹⁴M. Cho *et al.*, *Appl. Phys. Lett.* **106**, 181107 (2015).
- ¹⁵W. Peng, M. M. Roberts, E. P. Nordberg, F. S. Flack, P. E. Colavita, R. J. Hamers, D. E. Savage, M. G. Lagally, and M. A. Eriksson, *Appl. Phys. Lett.* **90**, 183107 (2007).
- ¹⁶W. Zhou *et al.*, *Prog. Quantum Electron.* **38**, 1 (2014).
- ¹⁷K. Zhang, J.-H. Seo, W. Zhou, and Z. Ma, *J. Phys. D: Appl. Phys.* **45**, 143001 (2012).
- ¹⁸R. Shimokawa, M. Yamanaka, and I. Sakata, *Jpn. J. Appl. Phys.* **46**, 7612 (2007).
- ¹⁹A. F. Oskooi, D. Roundy, M. Ibanescu, P. Bermel, J. D. Joannopoulos, and S. G. Johnson, *Comput. Phys. Commun.* **181**, 687 (2010).